Viscoelastic Necking Dynamics Between Attractive Microgels

Shensheng Chen,[†,‡] Emad Pirhadi,[†] and Xin Yong[*,†]

†*Department of Mechanical Engineering, Binghamton University, The State University of New York, Binghamton, New York 13902, USA*

‡*Current Address: Division of Chemistry and Chemical Engineering,1200 E California Blvd, California Institute of Technology, Pasadena, California 91125, USA*

E-mail: xyong@binghamton.edu

Abstract

Hypothesis **:** Microgels can deform and interpenetrate and display colloid/polymer duality. The effective interaction of microgels in the collapsed state is governed by the interplay of polymer-solvent interfacial tension and bulk elasticity. A connecting neck is shown to mediate microgel interaction but its temporal evolution has not been addressed. We hypothesize that the necking dynamics of attractive microgels exhibits liquid-like or solid-like behavior over different time and length scales.

Experiments **:** We simulate the merging and pinching of attractive microgels with different crosslinking densities in explicit solvent using dissipative particle dynamics. The temporal coalescence dynamics of microgels is investigated and compared with simple liquid and polymeric droplets. We model the neck growth on long time scales using Maxwell model of polymer relaxation and compare the theoretical prediction with simulation data. The mechanical strength of the neck is characterized systematically via simulated pinch-off of microgels by steered molecular dynamics.

Findings **:** We evidence a crossover in the coalescence dynamics reflecting the viscoelastic signature of microgels. In contrast to the common knowledge that viscoelastic materials respond elastically on short time scales, the early expansion of the microgel neck exhibits a linear behavior, similar to the viscous coalescence of liquid droplets. However, the late regime with arrested dynamics resembles sintering of solid particles. Through an analytical model relating microgel dynamics to neck growth, we show that the long-term behavior is governed by stress relaxation of the polymers in the neck region and predict an exponential decay in the rate of growth, which agrees favorably with the simulation. Different from coalescence, the thread thinning in microgel breakup primarily highlights its polymeric characteristics.

Keywords: Attractive microgels; Viscoelasticity; Droplet coalescence; Dissipative particle dynamics; Maxwell model

Introduction

Microgels are macromolecular particles of sizes from nanoscale to microscale, which can swell or collapse in solution in response to changes in the external environment such as solvency, pH, ionic strength, and temperature.[1,2] The unique combination of shape-morphability and bio-compatibility makes microgels appealing for innovative applications in nanotechnology, biosensing, and drug delivery in which conventional colloid particles would fail.[1–4] In the collapsed state, microgels are found to be strongly attractive to each other upon contact due to predominant surface tension effect.[5–8] This adhesive contact could have significant influences on self-assembly, gelation, jamming, and pattern formation of microgel systems. In particular, the detailed dynamics of attraction could play an important role in governing the rheological behavior of microgel suspensions.[9,10] Thus, a mechanistic understanding of adhesion dynamics can enable experimentalists to prepare and exploit microgel materials with tailored properties. However, it has remained challenging to experimentally resolve contact dynamics and coalescence mechanisms of microgels on submicron spatiotemporal

scales,[11,12] which leaves clear opportunities for further exploration using numerical and theoretical methods.[13,14]

As a hallmark of polymeric materials, viscoelasiticity is expected to affect the merging of microgels in a fundamental way. The existence of internal or interfacial structures of viscoelastic droplets can generate elastic resistance that offsets surface tension and prevents them from full coalescence.[15–18] Similar behavior has been observed in the partial sintering of polymer particles.[19] Recent simulations reveal that microgel coalescence is mediated by the expansion of a connecting bridge (neck) like in Newtonian droplets[12,13,20–22] but the evolution is arrested, resulting in a dumbbell morphology.[8] Nevertheless, the effects of network structure and chain relaxation on the temporal dynamics of neck growth are still elusive.

Methods

We numerically investigate the merging and pinching dynamics of two attractive microgels in solution using dissipative particle dynamics (DPD) simulations.[8,23–28] Microgels are constructed as spherical polymer particles sculpted from an infinite tetra-functional network. Each polymer strand is modeled as a string of coarse-grained polymer beads with bond and angle potentials, and uniform length throughout the network. The bond and angle parameters are carefully chosen to avoid unphysical chain crossing. The crosslinking density of the microgel is controlled by the strand length. The important effects of the surrounding medium on liquid droplet coalescence have been well documented.[12,29] In order to properly capture the hydrodynamic effects, the surrounding medium is explicitly simulated in our system by the introduction of solvent beads. The interactions between polymer and solvent beads are relatively unfavorable, which represents poor solvent conditions.[8] The poor solvency yields collapsed microgels of approximately 20 nm in radius regardless of crosslinking densities. The size of the model microgel is thus experimentally relevant. Our model is parameterized to represent the widely-used thermoresponsive poly(N-isopropylacrylamide)(PNIPAM) mi-

crogels dispersed in water at temperatures around 60 °C,[8] which is above its volume phase transition temperature around 32 °C. Under this condition, the collapsed microgels become attractive to each other.[5–9] Simulation data are collected from five independent runs for each system of interest. A typical simulation of our system takes approximately 48 hours by using 4 Nvidia Tesla P100 GPU along with 4 Intel Xeon ES-2695 v4 CPU (72 CPU cores at 2.10 GHz). Neck radius quantification and additional simulation details are described in Supplementary Material. While exploring the microgel size effect is of general interest, DPD simulations of large microgels require a significant amount of computational resources and are left to future study.

Results and Discussion

Temporal coalescence dynamics

To highlight the distinct behaviors of microgel necking, we simulate two reference systems with one being simple liquid droplets composed by monomer beads, and another being polymer droplets of short linear chains ($N = 10$). The necking process of attractive microgels with a strand length equal to the chain length in the polymer droplets is simulated for comparison. Figure 1(a) shows both simple liquid and polymeric droplets coalesce into well mixed droplets, while the microgels only adhere to each other through a stable neck. The arrested coalescence of microgels underscores the importance of elastic effects as a result of polymer network deformation. Figure 1(b) shows the temporal evolution of the neck growth in simple liquid droplets reproduces the characteristic viscous ($r^* \sim \tau$) to inertial ($r^* \sim \tau^{1/2}$) transition.[11,12,30] Here, τ is the simulation time scale and r^* is a dimensionless neck radius defined by $r^* = r/R_g^0$, where R_g^0 is the radius of gyration of the droplet before contact. Interestingly, all three systems show linear neck expansion ($\sim \tau$) on short time scales. Learned from previous studies on the Newtonian coalescence of viscous droplets, this common regime indicates that the viscous effect dominates at early stages of coalescence.

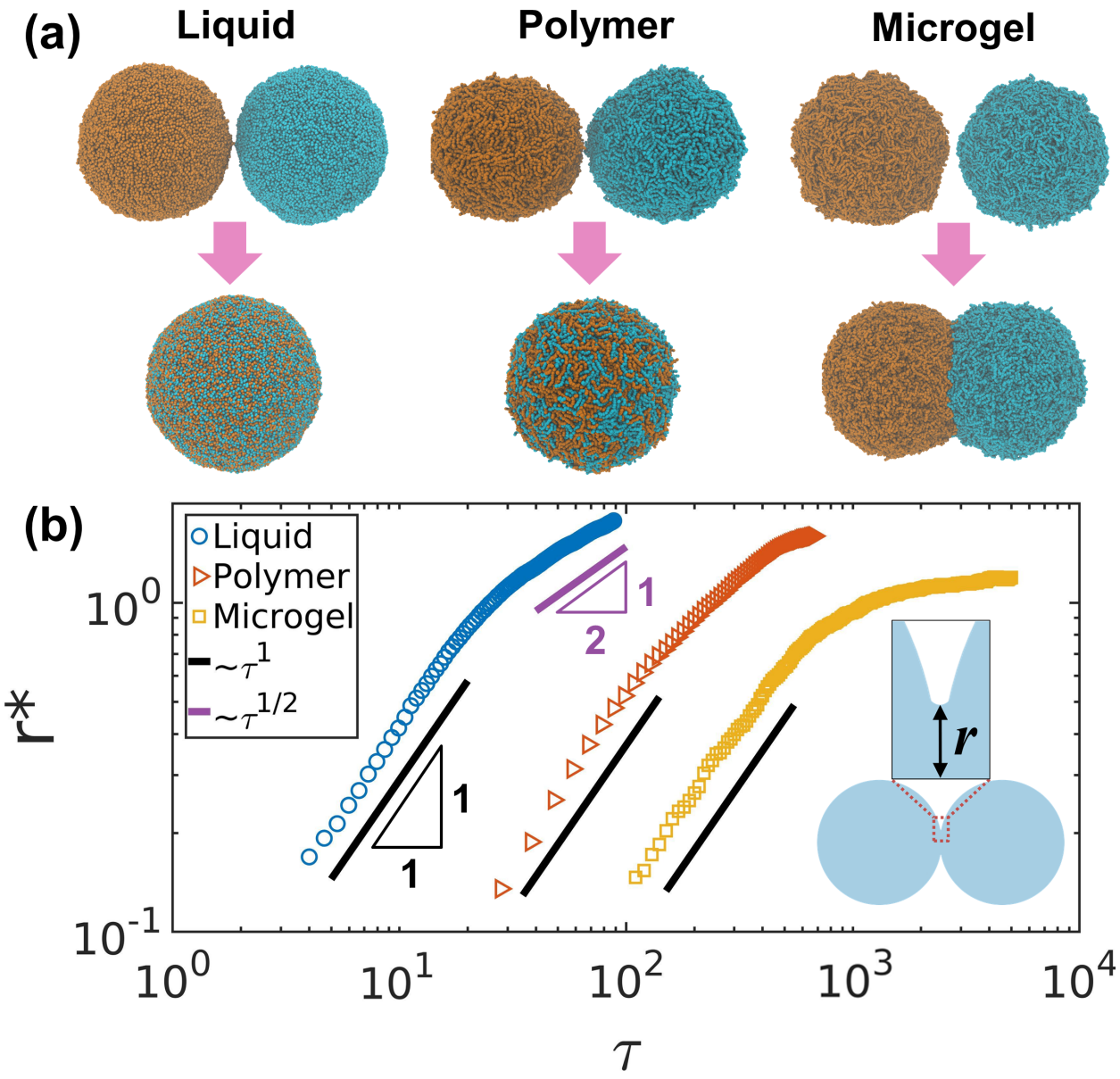

Figure 1: (a) Representative simulation snapshots before and after the complete evolution of the necks between pairs of simple liquid droplets, polymer droplets, and attractive microgels. Unlike the simple liquid and polymeric droplets, microgels do not coalesce. Notably, the snapshots in the two rows are not scaled to their actual sizes in the simulations, and the solvent beads are not shown for clarity. (b) Corresponding necking dynamics of the three systems presented in (a). All three systems show the linear viscous regime, but microgel neck expansion is significantly slower than the Newtonian and polymer droplets, especially on long time scales. Standard deviations among independent runs are small and not shown in the plot. The triangles with numbers indicate the slopes of fitting lines. The inset is a zoomed-in schematic of the neck region between two merging microgels.

The short-chain polymers are slightly more viscous compared to monomers. Thus, the neck growth of polymer droplets is slower than the simple liquid droplets but the scaling relation remains linear on short time scales.[31] On long time scales, polymer droplets show sublinear dynamics, which is qualitatively consistent with recent experiments.[32,33] In contrast to simple liquid and polymeric droplets, microgels exhibit a unique late-time contact dynamics. The rate of the neck growth decreases significantly over time and the neck development eventually ceases.

The early dynamics of polymeric droplets and microgels observed in our simulations is counterintuitive because viscoelastic spheres should behave like elastic solid on a short time scale of interest.[34,35] In addition, our data is in contrast to few recent studies on coalescence dynamics of polymer droplets[32,33,36] reporting power-law coalescence. Nevertheless, the dimensional neck radii of microgels at the early stage of coalescence would be on the order of a few nanometers. At such small length scales, the continuum mechanical description of viscoelasticity may be inapplicable and such a nanoscopic neck itself may not be readily realizable and accessible in physical experiments.[13] We contend that strain during the initial expansion is localized at the droplet/microgel surface and is too small to induce substantial conformation change of polymer chains. The strain response thus primarily depends on the viscous behavior of these surface chains. This could explain slower growth observed and the neck growth closely follows the dynamics of Newtonian coalescence.

Visco-to-viscoelastic crossover

The necking dynamics of microgels with crosslinking densities of $\psi = 1\%, 3\%, 5\%, 7\%$, and 11% are shown in Fig. 2. We observe a reasonable collapse of data for all the microgels during early stages of coalescence. The consistent linear expansion again confirms that microgels behave like liquid droplets on short time scales. The crosslinking density has no notable effects on the neck growth in this regime. The late dynamics however is modulated by the crosslinking density. The neck growth rate decays faster for microgels with higher

crosslinking densities. The final neck radius measured at the completion of adhesion also decreases monotonically. Clearly, the long-time evolution of the neck is governed by the elastic response of microgel. Based on these results, we hypothesize a separation in time scales in coalescence dynamics, which is dictated by a crossover time τ_0. On short time scales $\tau < \tau_0$, the necking exhibits the Newtonian behavior governed by the viscosity-capillarity competition. The surface polymer chains flow into the neck region without experiencing chain deformation and the topological constraint from the network connectivity. On long time scales $\tau > \tau_0$, the elastic resistance to further growth becomes prominent as the expansion now not only involves the motion of concentrated polymer chains in the neck region but also entails the network deformation in the bulk of microgel. We anticipate that the polymer chain relaxation plays an important role in this regime, which we term as viscoelastic regime. We model the transient contact dynamics in this regime by connecting microgel equation of motion to neck expansion.

Theoretical analysis of viscoelastic necking dynamics

We consider the necking of two microgels of the same size is symmetric in the approaching axis that connects the centers of mass of the microgels. The 1-D dynamics of one microgel approaching another can be described by the Langevin equation:

$$m\frac{\partial v}{\partial \tau} = -\zeta v - \frac{\partial U}{\partial x} + f \tag{1}$$

where m is the mass of microgel, v is the approaching velocity, and ζ is the friction coefficient. U is the interaction potential and x is the approaching coordinate with the origin defined at the mid-plane of the neck. f is a random force capturing thermal fluctuations, which satisfies the fluctuation-dissipation theorem.[37] Using Stokes-Einstein relation, we can estimate the momentum and diffusion time scales of microgel motion as $\tau_m = \frac{2\rho R^2}{9\eta}$ and $\tau_d = \frac{24\pi\eta R^3}{k_{\mathrm{B}}T}$, respectively. Here, ρ, R, η and $k_{\mathrm{B}}T$ are the solvent density, equilibrium microgel radius,

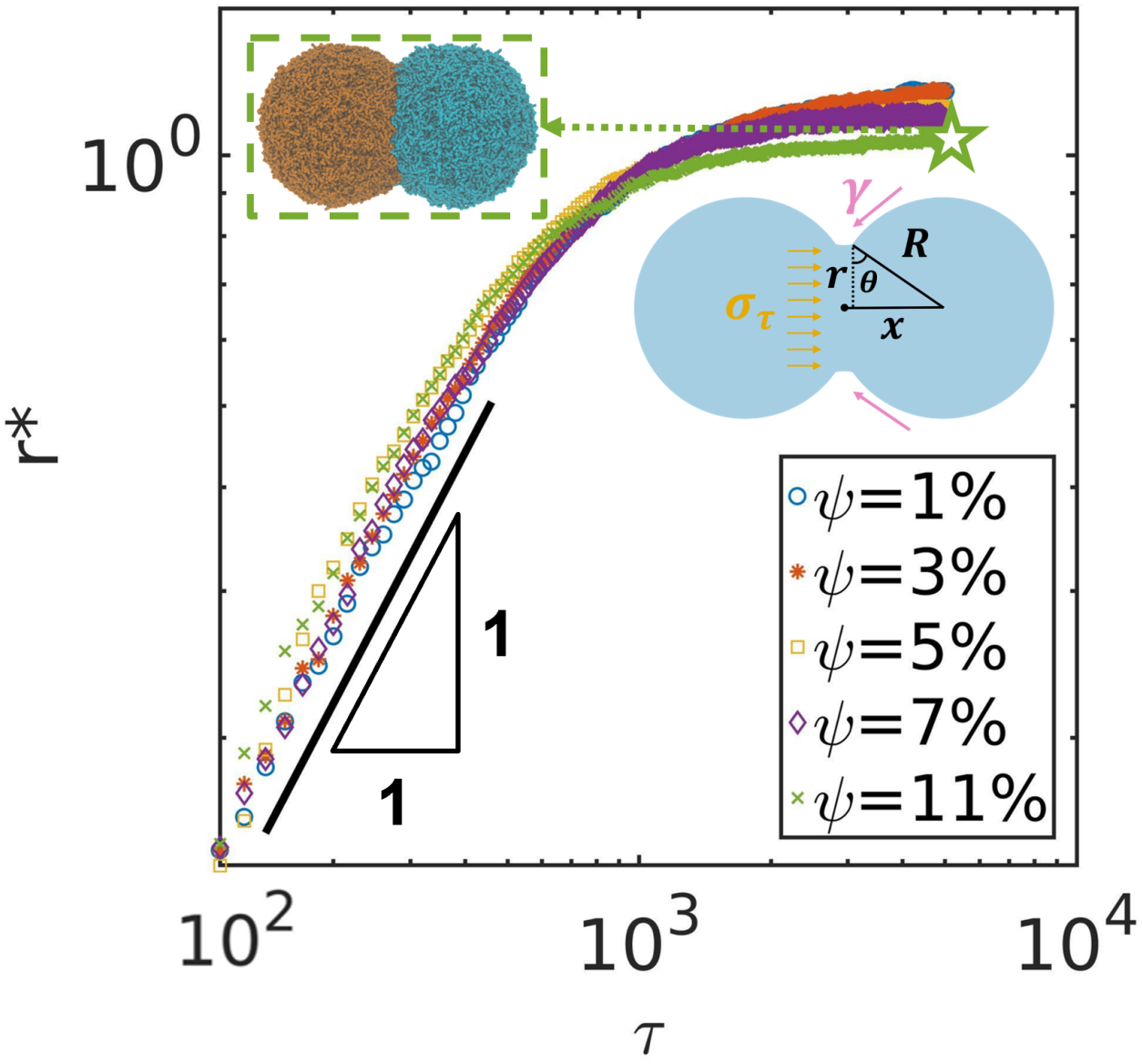

Figure 2: Necking dynamics of microgels with different crosslinking densities. The inset snapshot corresponds to the final steady-state structures of microgels at $\psi = 3\%$ and $\psi = 11\%$. The inset schematic shows the model geometry and the balance between surface tension and elastic forces. The triangle with numbers indicates the slope of a fitting line.

solvent viscosity, and characteristic thermal energy. τ_m is much smaller than τ_d for a microgel of 20 nm radius suspended in water in the standard temperature range of volume phase transition. Therefore, the inertia of the microgel can be ignored and only the overdamped dynamics is resolved. We also neglect the random force term f given that it is much smaller than the interaction force at the late time of neck evolution.[8] The equation is now simplified to $0 = -\zeta v - \frac{\partial U}{\partial x}$. As shown in Ref.[11] assuming the axisymmetric flow, the approaching velocity of microgels $v = dx/d\tau$ can be related to the neck growth velocity by $v \approx 0.5\, dr/d\tau$. The force derived from the interaction potential U has two components: the surface tension force that promotes adhesion and drives the neck expansion and the elastic force in the neck that arrests further growth. The surface force applied on one particle can be approximated by $\gamma \cdot 2\pi r \cdot \cos\theta = \gamma \cdot 2\pi r \cdot r/R$, where γ is gel-solvent surface tension. The elastic resistance is given by $\pi r^2 \cdot \sigma_\tau$, where σ_τ is the stress in the cross section of the neck. The equation of motion can now be cast in terms of the neck radius:

$$\zeta \frac{dr}{d\tau} = -\sigma_\tau \cdot \pi r^2 + \gamma \cdot 2\pi r \cdot \frac{r}{R} \tag{2}$$

In this study, we assume the deformation of collapsed microgel is small and treat R as a constant. The friction is mainly attributed to the Stokes drag of individual polymer chains at the interface of the two microgels, so the friction would scale with the neck area: $\zeta = \zeta_0 \pi r^2$. Supposing the elastic modulus of the microgel is G_τ, we have $\sigma_\tau = G_\tau \lambda$, where λ is the effective strain of the microgel. Considering small overall deformation during this necking regime, λ is also assumed to be a constant. By canceling the area dependence in all term, the equation becomes:

$$a \frac{dr}{d\tau} = -G_\tau + \frac{2\gamma}{\lambda R} \tag{3}$$

where $a = \zeta_0/\lambda$ is a scaling constant with units of $[\eta \cdot \tau]$.

The elastic stress is composed of a contribution from the bulk network deformation and the one from the concentrated polymers in the neck region. We can thus express the total

modulus G_τ into a time dependent part $G(\tau)$ that accounts for the polymer viscoelasticity in the neck, and a constant part G_{net} describing the intrinsic network elasticity: $G_\tau = G(\tau) + G_{net}$. G_{net} is a constant that only depends on network properties. The affine network model predicts $G_{net} = 3\rho_p k_\mathrm{B} T/N$, where ρ_p is polymer density inside the gel and N is the strand length.[38] Integrating the equation $a\frac{dr}{d\tau} = -G(\tau) - G_{net} + \frac{2\gamma}{\lambda R}$ from $\tau = \tau_0$ to $\tau = \infty$ should yield the necking dynamics in the long time regime. Moreover, this equation can be further simplified by noting the finite neck radius $r(\tau = \infty) = r_{end}$ at the steady state, which means the constant terms $-G_{net}$ and $\frac{2\gamma}{\lambda R}$ should cancel each other. This result can be understood by the balance between the network elasticity and capillarity at the steady state. Assuming the neck growth is a quasi-steady process during the late-stage adhesion, the cancellation of bulk elasticity and surface tension effect is valid at any instance. This treatment was also used in a recent theoretical analysis of Newtonian droplet coalescence.[30] Now we have

$$a\frac{dr}{d\tau} = -G(\tau) \tag{4}$$

$G(\tau)$ is essentially a dynamic elastic modulus associated with the viscoelastic relaxation of accumulated polymers in the neck area, which decays over time. Using the Maxwell model $G(\tau) = G_0 \cdot \exp(-\tau/\tau_c)$, where G_0 is a constant elastic modulus at $\tau = \tau_0$, and τ_c is the characteristic relaxation time of the polymers, the necking dynamics in the regime of $\tau > \tau_0$ can be obtained as

$$r = r_{end} - \tau_c b \cdot \exp(\frac{-\tau}{\tau_c}) \tag{5}$$

where $b = G_0/a$ and τ_c are fitting parameters.

The prediction of this model shows favorable agreement with our simulation data, as shown in the individual fittings in Fig. S1(a). The variations in the polymer relaxation time τ_c and the corresponding neck radius r_c for microgels of different crosslinking densities are given in Fig. S1(b). Generally, microgels with lower crosslinking densities (longer polymer strands) have larger τ_c and r_c. The trend of variations for τ_c qualitatively agrees with the

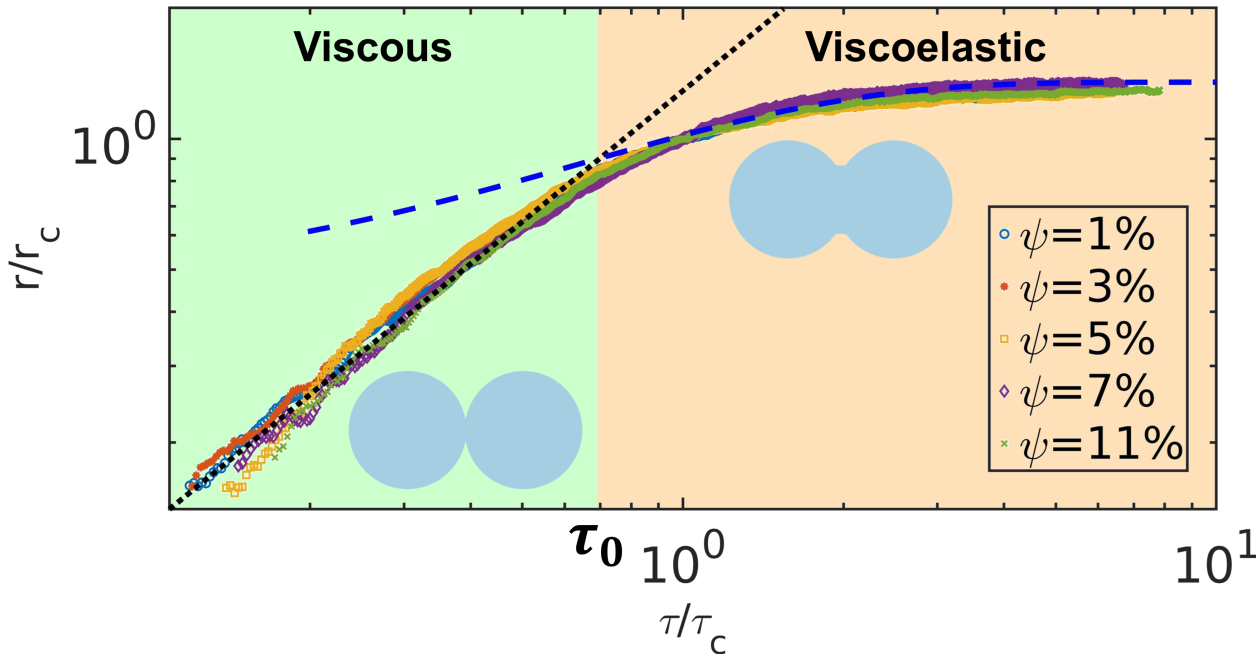

Figure 3: Normalized necking growth r/r_c as a function of normalized time τ/τ_c. The characteristic relaxation time of each microgel τ_c is obtained from the fitting to Eq.(5). Black dotted line corresponds to the early linear scale relaxation($\sim \tau/\tau_c$) and blue dashed curve represents the late dynamics modeled by Eq.(5). The intersection of the two fitting curves determines the crossover time τ_0.

Rouse model prediction $\tau_c \sim N^{-2}$. However, polymer chains in microgels are connected by crosslinkers, we do not expect it follows the exact Rouse scaling. Note that the difference in τ_c between low crosslinkers 1% and 3% is small, which is probably caused by the entanglement effect for long polymer chains. If we normalize the necking radius by r/r_c and time by τ/τ_c, the simulation data for all five microgels collapse reasonably on one master curve, as shown in Fig. 3. The crossover between the viscous and viscoelastic regimes is presented by a crossover time τ_0, which is dictated by the intersection of the curve given by Eq. (5) and the linear fitting of the viscous regime. This results provides evidence for the separation of regimes in microgel neck growth and the dominant effect of polymer relaxation on the late-stage dynamics.

Our simulation results and theoretical model show a transition from a viscous regime to a viscoelastic regime in microgel necking. To verify this new insight, experiments are needed to measure some key observations, for example the crossover time τ_0. Previous experimental studies[11,30,39] reported that the crossover (from viscous to inertial regime) time of liquid droplet coalescence scales with the square root of droplet size $\sqrt{R}$, and thus increases as the droplet size increases. Although we have yet to obtain a theoretical prediction of τ_0, the results imply its dependence on the fluid-like behavior of microgel in the viscous regime. Thus, while the crossover time τ_0 for the microgels in this study may be too small for experimental measurements, we expect τ_0 of larger microgels to be measurable by current experimental techniques. For example, the sintering dynamics of sub-micro polymeric particles have been be measured by 3D tomography, nanoindentation and confocal microscopy.[40]

The polymer strands used in this work are relatively short ($N = 4 - 50$). Thus the entanglement of polymers is expected to have minor effects on the chain dynamics. As a result, the Maxwell model, a special case of the Rouse model[38] with equal modes, serves well here for describing the polymer relaxation in the long-time viscoelastic regime. We envision the use of more sophisticated and accurate Rouse model would push the solution success toward earlier times, as it involves multi-mode relaxation on different time scales. However,

the analytical solution of using Rouse model will be non-trivial. The Eq.(5) based on Maxwell relaxation provides a simple and elegant prediction for microgel necking dynamics in the long time regime.

Pinching of attractive microgels

It is also of interest to explore the strength of the neck between these attractive microgels. To investigate the adhesive properties of microgel neck, we model the breakup of microgels by pulling them apart at a constant speed using steered molecular dynamics (SMD) simulation.[8] Figure 4(a) shows that the two microgels produce a long and stable neck prior to it ruptures. This behavior is reminiscent of elasto-capillary thinning and breakup of viscoelastic droplets.[36,41,42] The necking radius variations shown in Fig. 4(b) demonstrate microgels with low crosslinking densities can endure greater separation and requires more mechanical work for eventual pinch-off (Fig. 4(d)). To quantify the microgel morphology during pinch-off, we calculate the gyration tensor $\mathbf{S}_{mn} = (1/N)\sum_{i=1}^{N}(r_m^{(i)} - r_m^{CM})(r_n^{(i)} - r_n^{CM})$, where $r_m^{(i)}$ is the m^{th} Cartesian coordinate of the position vector of the i^{th} constituent DPD bead of the microgel. Figure 4(c) shows nonmonotonic microgel deformation quantified by the principal moment of gyration tensor in the pulling direction λ_x^2, which characterizes the deformation along the pulling direction. This behavior indicates that the microgels start to recover their shape before their necks completely break. Our results confirm microgels with low ψ are more liquid-like and the adhesion between them is stronger[1,8] as a result of dominant surface tension effect.

The pinching behavior also provides important information on the interplay among inertia, surface tension, interparticle interaction, and microgel structure. The longer endurance of neck at lower crosslinking densities implies that the surface tension exhibit a dominant effect on the contact of these fluid-like microgels. They are able to maintain the neck even after the shape recovery begins. On the other hand, the early break of highly crosslinking microgels highlights the importance of inertia and elasticity for relatively rigid particles.

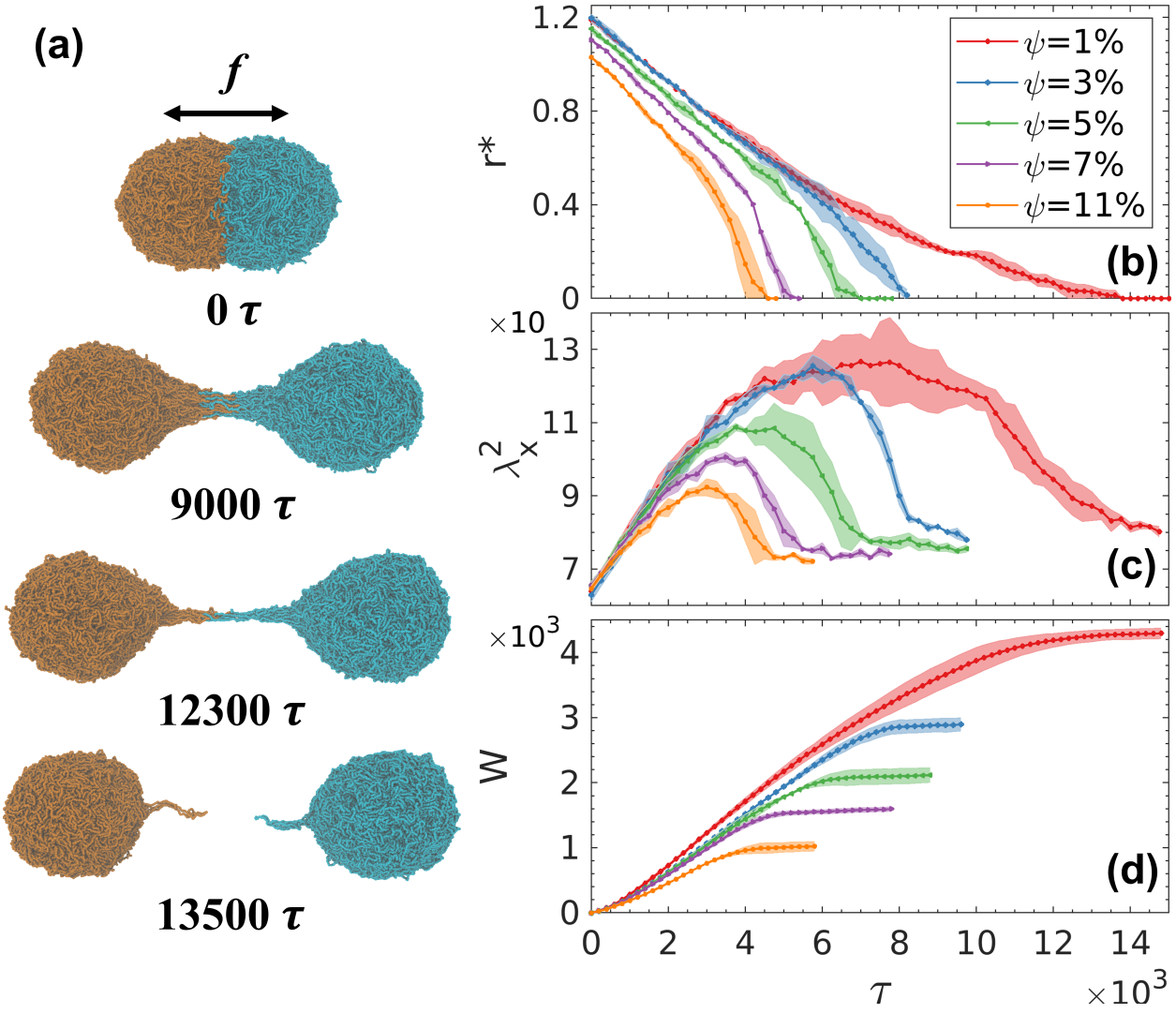

Figure 4: (a) Represented snapshots showing the formation of elongated thread during the pinch-off of microgels with $\psi = 1\%$. (b) Neck radius changes over time during the breakup of microgels with varies crosslinking densities. (c) Variations in the principal moment of gyration tensor of the microgels in the direction of pulling coordinate λ_x^2. (d) Accumulated work during the pulling. The shaded area represents standard deviations of five independent runs. The spring constant and pulling speed is set to 5000 $k_B T/r_0^2$ and 0.0024 r_0/τ, where r_0 is the cut off interaction distance in DPD simulations.[8]

Conclusions

In summary, this work presents the first attempt to explore the role of polymer viscoelasticity in determining the necking dynamics of attractive microgels in the collapsed state. In contrast to common expectation that elastic behavior of polymer sphere dominates on short time scales during coalescence,[35] the early dynamics of microgel necking is found to be surprisingly similar to viscous coalescence of Newtonian droplets.[12,30] On the long time scales, the necking dynamics is observed to be arrested by the network structure of microgels.[15] In this regime, the neck growth coincides with the relaxation of polymer chains in the neck. Based on the Maxwell polymer relaxation model, the simple theoretical prediction of late neck growth shows favorable agreement with the simulation data. The result suggests a novel viscous-to-viscoelastic crossover in the coalescence of strongly attractive microgels. On the other hand, the breakup of microgels is mediated by the formation of elongated polymer thread and subsequent thinning before eventual rupture. This pinch-off behavior largely highlights the polymeric nature of microgels. This work shed light on the intriguing interface dynamics of these emerging soft particles on different length and time scales.

In addition, the findings of this work provide useful insights for designing microgels with tailored properties in experiments. The correlation between the necking dynamics and polymer relaxation suggests that the rheology of attractive microgels depends sensitively on the density and length of polymer chains at the surface of the microgel. Consequently, the rheology of microgel suspensions can be controlled by modifying network structure or grafting dangling chains at the microgel surface. Moreover, the characterization of the pinching behavior shows that microgels with lower crosslinking densities dissipate more work and endure stronger deformation. This result sheds light on the manipulation of the interplay among inertia, elasticity, and capillarity in microgel materials through tuning interfacial chain structure.

Acknowledgement

We gratefully acknowledge funding from the National Science Foundation under Grant No. CMMI-1939362 for partial support of this research. Generous allocation of computing time was provided by the Center for Functional Nanomaterials, which is a U.S. DOE Office of Science Facility, at Brookhaven National Laboratory under Contract No. DESC0012704.

References

(1) Plamper, F. A.; Richtering, W. Functional Microgels and Microgel Systems. *Accounts of Chemical Research* **2017**, *50*, 131–140.

(2) Seiffert, S.; Thiele, J.; Abate, A. R.; Weitz, D. A. Smart Microgel Capsules from Macromolecular Precursors. *Journal of the American Chemical Society* **2010**, *132*, 6606–6609.

(3) Saxena, S.; Hansen, C. E.; Lyon, L. A. Microgel Mechanics in Biomaterial Design. *Accounts of Chemical Research* **2014**, *47*, 2426–2434.

(4) Seiffert, S. Small but Smart: Sensitive Microgel Capsules. *Angewandte Chemie International Edition* **2013**, *52*, 11462–11468.

(5) Wu, J.; Huang, G.; Hu, Z. Interparticle Potential and the Phase Behavior of Temperature-Sensitive Microgel Dispersions. *Macromolecules* **2003**, *36*, 440–448.

(6) Stieger, M.; Pedersen, J. S.; Lindner, P.; Richtering, W. Are Thermoresponsive Microgels Model Systems for Concentrated Colloidal Suspensions? A Rheology and Small-Angle Neutron Scattering Study. *Langmuir* **2004**, *20*, 7283–7292.

(7) Romeo, G.; Fernandez-Nieves, A.; Wyss, H. M.; Acierno, D.; Weitz, D. A. Temperature-Controlled Transitions Between Glass, Liquid, and Gel States in Dense p-NIPA Suspensions. *Advanced Materials* **2010**, *22*, 3441–3445.

(8) Chen, S.; Yong, X. Elastocapillary interactions of thermoresponsive microgels across the volume phase transition temperatures. *Journal of Colloid and Interface Science* **2021**, *584*, 275–280.

(9) Shao, Z.; Negi, A. S.; Osuji, C. O. Role of interparticle attraction in the yielding response of microgel suspensions. *Soft Matter* **2013**, *9*, 5492.

(10) Minami, S.; Watanabe, T.; Suzuki, D.; Urayama, K. Viscoelasticity of dense suspensions of thermosensitive microgel mixtures undergoing colloidal gelation. *Soft Matter* **2018**, *14*, 1596–1607.

(11) Paulsen, J. D.; Burton, J. C.; Nagel, S. R. Viscous to Inertial Crossover in Liquid Drop Coalescence. *Physical Review Letters* **2011**, *106*, 114501.

(12) Paulsen, J. D.; Carmigniani, R.; Kannan, A.; Burton, J. C.; Nagel, S. R. Coalescence of bubbles and drops in an outer fluid. *Nature Communications* **2014**, *5*, 3182.

(13) Perumanath, S.; Borg, M. K.; Chubynsky, M. V.; Sprittles, J. E.; Reese, J. M. Droplet Coalescence is Initiated by Thermal Motion. *Physical Review Letters* **2019**, *122*, 104501.

(14) Anthony, C. R.; Harris, M. T.; Basaran, O. A. Initial regime of drop coalescence. *Physical Review Fluids* **2020**, *5*, 033608.

(15) Pawar, A. B.; Caggioni, M.; Hartel, R. W.; Spicer, P. T. Arrested coalescence of viscoelastic droplets with internal microstructure. *Faraday Discussions* **2012**, *158*, 341.

(16) Dahiya, P.; Caggioni, M.; Spicer, P. T. Arrested coalescence of viscoelastic droplets: polydisperse doublets. *Philosophical Transactions of the Royal Society A: Mathematical, Physical and Engineering Sciences* **2016**, *374*.

(17) Studart, A. R.; Shum, H. C.; Weitz, D. A. Arrested Coalescence of Particle-coated Droplets into Nonspherical Supracolloidal Structures. *The Journal of Physical Chemistry B* **2009**, *113*, 3914–3919.

(18) Ata, S. Coalescence of Bubbles Covered by Particles. *Langmuir* **2008**, *24*, 6085–6091.

(19) Hejmady, P.; van Breemen, L. C. A.; Anderson, P. D.; Cardinaels, R. Laser sintering of polymer particle pairs studied by in situ visualization. *Soft Matter* **2019**, *15*, 1373–1387.

(20) Aarts, D. G. A. L.; Lekkerkerker, H. N. W.; Guo, H.; Wegdam, G. H.; Bonn, D. Hydrodynamics of Droplet Coalescence. *Physical Review Letters* **2005**, *95*, 164503.

(21) Sadeghi, H. M.; Sadri, B.; Kazemi, M. A.; Jafari, M. Coalescence of charged droplets in outer fluids. *Journal of Colloid and Interface Science* **2018**, *532*, 363–374.

(22) Rekvig, L.; Frenkel, D. Molecular simulations of droplet coalescence in oil/water/surfactant systems. *The Journal of Chemical Physics* **2007**, *127*, 134701.

(23) Groot, R. D.; Warren, P. B. Dissipative particle dynamics: Bridging the gap between atomistic and mesoscopic simulation. *The Journal of Chemical Physics* **1997**, *107*, 4423–4435.

(24) Español, P.; Warren, P. B. Perspective: Dissipative particle dynamics. *The Journal of Chemical Physics* **2017**, *146*, 150901.

(25) Chen, S.; Yong, X. Dissipative particle dynamics modeling of hydrogel swelling by osmotic ensemble method. *The Journal of Chemical Physics* **2018**, *149*, 094904.

(26) Hoppe Alvarez, L.; Eisold, S.; Gumerov, R. A.; Strauch, M.; Rudov, A. A.; Lenssen, P.; Merhof, D.; Potemkin, I. I.; Simon, U.; Wöll, D. Deformation of Microgels at Solid–Liquid Interfaces Visualized in Three-Dimension. *Nano Letters* **2019**, *19*, 8862–8867.

(27) Camerin, F.; Gnan, N.; Rovigatti, L.; Zaccarelli, E. Modelling realistic microgels in an explicit solvent. *Scientific Reports* **2018**, *8*, 14426.

(28) Akella, V.; Gidituri, H. Universal scaling laws in droplet coalescence: A dissipative particle dynamics study. *Chemical Physics Letters* **2020**, *758*, 137917.

(29) Baroudi, L.; Nagel, S. R.; Morris, J. F.; Lee, T. Dynamics of viscous coalescing droplets in a saturated vapor phase. *Physics of Fluids* **2015**, *27*, 121702.

(30) Xia, X.; He, C.; Zhang, P. Universality in the viscous-to-inertial coalescence of liquid droplets. *Proceedings of the National Academy of Sciences* **2019**, *116*, 23467–23472.

(31) Yao, W.; Maris, H. J.; Pennington, P.; Seidel, G. M. Coalescence of viscous liquid drops. *Physical Review E* **2005**, *71*, 016309.

(32) Varma, S. C.; Saha, A.; Mukherjee, S.; Bandopadhyay, A.; Kumar, A.; Chakraborty, S. Universality in coalescence of polymeric fluids. *Soft Matter* **2020**, *16*, 10921–10927.

(33) Sivasankar, V. S.; Etha, S. A.; Hines, D. R.; Das, S. Coalescence of Microscopic Polymeric Drops: Effect of Drop Impact Velocities. *Langmuir* **2021**, *37*, 13512–13526.

(34) Jagota, A.; Argento, C.; Mazur, S. Growth of adhesive contacts for Maxwell viscoelastic spheres. *Journal of Applied Physics* **1998**, *83*, 250–259.

(35) Lin, Y.; Hui, C.; Jagota, A. The Role of Viscoelastic Adhesive Contact in the Sintering of Polymeric Particles. *Journal of Colloid and Interface Science* **2001**, *237*, 267–282.

(36) Dekker, P. J.; Hack, M. A.; Tewes, W.; Datt, C.; Bouillant, A.; Snoeijer, J. H. When Elasticity Affects Drop Coalescence. *Physical Review Letters* **2022**, *128*, 028004.

(37) Prost, J.; Joanny, J.-F.; Parrondo, J. M. R. Generalized Fluctuation-Dissipation Theorem for Steady-State Systems. *Physical Review Letters* **2009**, *103*.

(38) Michael, R.; Ralph H, C. *Polymer Physics*, 1st ed.; Oxford University Press, 2003.

(39) Burton, J. C.; Taborek, P. Role of Dimensionality and Axisymmetry in Fluid Pinch-Off and Coalescence. *Physical Review Letters* **2007**, *98*.

(40) Fuchs, R.; Weinhart, T.; Ye, M.; Luding, S.; Butt, H.-J.; Kappl, M. Initial stage sintering of polymer particles – Experiments and modelling of size-, temperature- and time-dependent contacts. *EPJ Web of Conferences* **2017**, *140*, 13012.

(41) Anna, S. L.; McKinley, G. H. Elasto-capillary thinning and breakup of model elastic liquids. *Journal of Rheology* **2001**, *45*, 115–138.

(42) Yang, J.; Xu, Y. Coalescence of two viscoelastic droplets connected by a string. *Physics of Fluids* **2008**, *20*, 043101.